

Highlights in the study of exoplanet atmospheres

Adam S. Burrows¹

Exoplanets are now being discovered in profusion. To understand their character, however, we require spectral models and data. These elements of remote sensing can yield temperatures, compositions and even weather patterns, but only if significant improvements in both the parameter retrieval process and measurements are made. Despite heroic efforts to garner constraining data on exoplanet atmospheres and dynamics, reliable interpretation has frequently lagged behind ambition. I summarize the most productive, and at times novel, methods used to probe exoplanet atmospheres; highlight some of the most interesting results obtained; and suggest various broad theoretical topics in which further work could pay significant dividends.

The modern era of exoplanet research started in 1995 with the discovery of the planet 51 Pegasi b¹, when astronomers detected the periodic radial-velocity Doppler wobble in its star, 51 Peg, induced by the planet's nearly circular orbit. With these data, and knowledge of the star, the orbital period (P) and semi-major axis (a) could be derived, and the planet's mass constrained. However, the inclination of the planet's orbit was unknown and, therefore, only a lower limit to its mass could be determined. With a lower limit of $0.47 M_J$ (where M_J is the mass of Jupiter) and given its proximity to its primary (a is about 0.052 AU, 1 AU being the Earth–Sun distance; one hundred times closer to its star than Jupiter is to the Sun), the induced Doppler wobble is optimal for detection by the radial-velocity technique. The question was how such a 'hot Jupiter' could exist and survive. Although its survival is now understood (see 'Winds from planets'), the reason for its close orbital position is still a subject of vigorous debate. Nevertheless, such close-in giants are selected for using the radial-velocity technique and soon scores, then hundreds, of such gas giants were discovered in this manner.

However, aside from a limit on planet mass, and the inference that proximity to its star leads to a hot (1,000–2,000 kelvin (K)) irradiated atmosphere, no useful physical information on such planets was available with which to study planet structure, their atmospheres or composition. A breakthrough along the path to characterization, and the establishment of mature exoplanet science, occurred with the discovery of giant planets, still close-in, that transit the disk of their parent star. The chance of a transit is larger if the planet is close, and HD 209458b, which is about 0.05 AU from its star, was the first to be found². Optical measurements yielded a radius for HD 209458b of about $1.36 R_J$, where R_J is the radius of Jupiter. Jupiter is roughly ten times, and Neptune is roughly four times, the radius of Earth (R_E). Since then, hundreds of transiting giants have been discovered using ground-based facilities. The magnitude of the attendant diminution of a star's light during such a primary transit (eclipse) by a planet is the ratio of their areas (the transit depth, R_p^2/R_*^2 , where R_p is the planet's radius and R_* is the star's radius), so with knowledge of the star's radius, the planet's radius can be determined. Along with radial-velocity data, because the orbital inclination of a planet in transit is known, one then has a radius–mass pair with which to do some science. The transit depth of a giant passing in front of a Sun-like star is about 1%, and such a large magnitude can easily be measured with small telescopes from the ground. A smaller,

Earth-like planet requires the ability to measure transit depths 100 times more precisely. It was not long before many hundreds of gas giants were detected both in transit and by the radial-velocity method, the former requiring modest equipment and the latter requiring larger telescopes with state-of-the-art spectrometers with which to measure the small stellar wobbles. Both techniques favour close-in giants, so for many years these objects dominated the bestiary of known exoplanets.

Better photometric precision near or below one part in 10^4 – 10^5 , which is achievable only from space, is necessary to detect the transits of Earth-like and Neptune-like exoplanets across Sun-like stars, and, with the advent of Kepler³ and CoRoT (Convection, Rotation and Planetary Transits)⁴, astronomers have now discovered a few thousand exoplanet candidates. Kepler in particular revealed that most planets are smaller than about $2.5 R_E$ (four times smaller than Jupiter), but fewer than around 100 of the Kepler candidates are close enough to us to be measured with state-of-the-art radial-velocity techniques. Without masses, structural and bulk compositional inferences are problematic. Moreover, most of these finds are too distant for photometric or spectroscopic follow-up from the ground or space to provide thermal and compositional information.

A handful of the Kepler and CoRoT exoplanets, and many of the transiting giants and 'sub-Neptunes' discovered using ground-based techniques, are not very distant and have been photometrically and spectroscopically followed up using both ground-based and space-based assets to help to constrain their atmospheric properties. In this way, and with enough photons, some information on atmospheric compositions and temperatures has been revealed for around 50 exoplanets, mostly giants. However, even these data are often sparse and ambiguous, rendering most such hard-won results provisional⁵. The nearby systems hosting larger transiting planets around smaller stars are the best targets for a programme of remote sensing to be undertaken, but such systems are a small subset of the thousands of exoplanets currently in the catalogues.

One method by which astronomers are performing such studies is by measuring the transit radius as a function of wavelength^{6–8}. Because the opacity of molecules and atoms in a planet's atmosphere is a function of wavelength, the apparent size of the planet is also a function of wavelength — in a manner that is characteristic of atmospheric composition. Such a 'radius spectrum' can reveal the atmosphere's composition near the planet terminators, but the magnitude of the associated variation is

¹Astrophysical Sciences, Princeton University, 4 Ivy Lane, Princeton, New Jersey 08544, USA.

down from the average transit depth by a factor of around $2H/R_p$, where H is the atmospheric scale height (a function of average temperature and gravity). This ratio can be ~ 0.1 to 0.01 , correspondingly making it more difficult to determine a transit radius spectrum. Only telescopes such as the Spitzer Space Telescope⁹, the Hubble Space Telescope and the largest ground-based telescopes with advanced spectrometers are up to the task, and even then the results can be difficult to interpret.

Another method probes the atmospheres of transiting exoplanets at secondary eclipse, when the star occults the planet about 180° out of phase with the primary transit. The abrupt difference between the summed spectrum of planet and star just before and during the eclipse of the planet by the star is the planet's spectrum at full face. Secondary eclipse spectra include reflected (mostly in the optical and near-ultraviolet region) and thermally emitted (mostly in the near- and mid-infrared region) light, and models are necessary to distinguish, if possible, the two components. It should be noted that separate images of the planet and star are not obtained by this technique, and a planet must be transiting. With few exceptions, when the planet does not transit, the summed light of a planet and star varies too slowly and smoothly for such a variation to be easily distinguished from the systematic uncertainties of the instruments to reveal the planet's emissions as a function of orbital phase. For the close-in transiting hot Jupiters, the planet flux in the near-infrared is 10^{-3} times the stellar flux — much higher than the ratio expected for the class of planet in a wide orbit that can be separated from its primary star by high-contrast imaging techniques (see 'High-contrast imaging'). In cases when such high-contrast direct imaging is feasible, the planet is farther away from the star (hence, dim) and difficult to discern from under the stellar glare. However, hot, young giants can be self-luminous enough to be captured by current high-contrast imaging techniques, and a handful of young giant planets have been discovered and characterized by this technique. More are expected as the technology matures^{10–13}.

The secondary eclipse and primary transit methods used to determine or constrain atmospheric compositions and temperatures (as well as other properties) generally involve low-resolution spectra with large systematic and statistical errors. These methods are complementary in that transit spectra reliably reveal the presence of molecular and atomic features, and are an indirect measure of temperature through the pressure-scale height, whereas the flux levels of secondary eclipse spectra scale directly with temperature, but could in fact be featureless for an isothermal atmosphere. The theoretical spectra with which they are compared in order to extract parameter values are also imperfect, and this results in less trustworthy information than one would like. Giant planets (and 'Neptunes') orbiting closely around nearby stars are the easiest targets, and are the stepping stones to 'Earths'. Secondary and primary transit spectral measurements of Earth-like planets around Sun-like stars, as well as direct high-contrast imaging of such small planets, are not currently feasible. However, measurements of exo-Earths around smaller M-dwarf stars might be, if suitable systems can be found. Nevertheless, with a few score of transit and secondary eclipse spectra, some planetary phase light curves, a few high-contrast campaigns and measurements, and some narrow-band, but very high spectral resolution measurements using large telescopes, the first generation of exoplanet-atmosphere studies has begun.

There are several helpful reviews on the theory of exoplanet atmospheres^{14–22}. Added to these, there are informed discussions on the molecular spectroscopy and opacities that are central to model building^{23–27}. Monographs on the relevant thermochemistry and abundances have been published over the years^{28–32}. In this Review, I do not attempt to cover the literature of detections and claims, nor do I attempt to review the thermochemical, spectroscopic or dynamical modelling efforts so far. Instead, I focus on those few results concerning exoplanet atmospheres that to my mind stand out, that seem most robust and that collectively summarize what we have truly learned. I present, of necessity, only a small subset of the published literature, and no doubt some compelling results have been neglected for lack of space. In addition, I

touch on only the basics of the atmosphere theory applied so far, preferring to focus, when possible, on the progress in theory that is necessary for the next generation of exoplanet-atmosphere studies to evolve productively. I embark on a discussion of what I deem to be a few of the milestone observational papers in core topics; these might be considered to constitute the spine of progress in recent exoplanet-atmosphere study. I accompany each with a short discussion of the associated theoretical challenges posed by the data.

Transit detection of atoms and molecules

The apparent transit radius of a planet with a gaseous atmosphere is the impact parameter of a ray of stellar light for which the optical depth at that wavelength (λ) is of order unity. It should be noted that at that level the corresponding radial optical depth, which if in absorption is relevant to emission spectra at secondary eclipse, will be much smaller. Because an atmosphere has a thickness (extent), and because absorption and scattering cross-sections are functions of photon wavelength that in combination with the air column constitute optical depth, the measured transit radius is a function of wavelength. Therefore, measurements of a planet's transit depths at many wavelengths of light reveal its atomic and molecular composition. A good approximation for this is given by³³:

$$dR_p/d\ln(\lambda) \sim H \ln \sigma(\lambda)/d\ln(\lambda) \quad (1)$$

where $\sigma(\lambda)$ is the composition-weighted total cross-section and the scale height, H , is $kT/\mu g$, where g is the planet's surface gravity, μ is the mean molecular weight, T is an average atmospheric temperature, and k is Boltzmann's constant. H sets the scale of the magnitude of potential fluctuations of R_p with λ , and $\sigma(\lambda)$ is determined mostly by the atomic and molecular species in the atmosphere.

Charbonneau *et al.*³⁴ were the first to successfully use this technique with the $4\text{-}\sigma$ measurement of atomic sodium in the atmosphere of HD 209458b. Along with HD 189733b, this nearby giant planet has been the most photometrically and spectroscopically scrutinized. Since then, Sing *et al.*³⁵ have detected potassium in XO-2b and Pont *et al.*^{36,37} have detected both sodium and potassium in HD 189733b. These are all optical measurements at and around the sodium D doublet (about $0.589 \mu\text{m}$) and the potassium resonance doublet (around $0.77 \mu\text{m}$), and reveal the telltale differential transit depths in and out of the associated lines.

Based on the study of brown dwarfs, the presence of neutral alkali metals in the atmospheres of irradiated exoplanets with similar atmospheric temperatures ($\sim 1,000\text{--}1,500 \text{ K}$) was expected, and their detection was gratifying. Indeed, there is a qualitative correspondence between the atmospheres of close-in and irradiated, or young giant planets (with masses of order M_J) and older brown dwarfs (with masses of tens of M_J). Alkalis persist to lower temperatures ($\sim 800\text{--}1,000 \text{ K}$) and are revealed in close-in exoplanet transit and emission spectra, and in older brown-dwarf emission spectra because silicon and aluminium, with which they would otherwise combine to form feldspars, are sequestered at higher temperatures and greater depths into more refractory species, and rained out. Had the elements with which sodium and potassium would have combined persisted in the atmosphere at altitude, these alkalis would have combined and their atomic form would not have been detected³⁸. The more refractory silicates (and condensed iron) reside in giant exoplanets (and in Jupiter and Saturn), but at great depths. In L-dwarf brown dwarfs, they are at the surface, reddening the emergent spectra significantly.

However, the strength, in transiting giant exoplanets, of the contrast in and out of these atomic alkali lines is generally less than expected⁸. Subsolar elemental sodium and potassium abundances, ionization by stellar light, and hazes have been invoked to explain the diminished strength of their associated lines, but the haze hypothesis is gaining ground. The definition of a haze can merge with that of a cloud, but generally hazes are clouds of small particulates at altitude that may be condensates of trace species or products of photolysis by stellar

ultraviolet light and polymerization. They are generally not condensates of common or abundant molecular species (such as water, ammonia, iron or silicates, none of which fits the bill here). Although it is not at all clear what this haze is, hazes at altitude (<0.01 bars) can provide a nearly featureless continuum opacity to light and easily mute atomic and molecular line strengths. Indeed, hazes are emerging as central and ubiquitous features in exoplanet atmospheres. Annoyingly, not much mass is necessary to have an effect on transit spectra, making quantitative interpretation all the more difficult. The fact that the red colour of Jupiter itself is produced by a trace species (perhaps a haze) that so far has not been identified is a sobering testament to the difficulties that lie ahead in completely determining exoplanet atmospheric compositions.

The multi-frequency transit measurements of HD 189733b from the near-ultraviolet to the mid-infrared by Pont *et al.*^{36,37} are the clearest and most marked indications that some exoplanets have haze layers (Fig. 1). Curiously, the measurements show no water or other molecular features in transit. Aside from the aforementioned sodium and potassium atomic features in the optical, the transit spectrum of HD 189733b is consistent with a featureless continuum. Water features in a hydrogen (H_2) atmosphere are very difficult to completely suppress, so their absence is strange. Furthermore, the transit radius increases below about $1.0\ \mu\text{m}$ with decreasing wavelength in a manner that is reminiscent of Rayleigh scattering. However, owing to the large cross-sections implied, the culprit can only be a haze or a cloud. It should be mentioned that these transit data cannot distinguish between absorption and scattering, although scattering is the more likely cause for most plausible haze materials and particle sizes. Scattering is also indicated by the near lack of evidence for absorbing particulates in HD 189733b secondary eclipse emission spectra³⁹. Together, these data suggest that a scattering haze layer at altitude is obscuring the otherwise distinctive spectral features of the spectroscopically active atmospheric constituents.

Transit spectra for the mini-Neptune GJ 1214b have been taken by many groups, but the results concerning possible distinguishing spectral features have, until recently, been quite ambiguous⁴⁰. In principle, there are diagnostic water features at around $1.15\ \mu\text{m}$ and $1.4\ \mu\text{m}$. However, Kreidberg *et al.*⁴¹, using the Wide Field Camera-3 (WFC3) on the Hubble Space Telescope, have demonstrated that from ~ 1.1 to $1.6\ \mu\text{m}$ its transit spectrum is around 5–10 times flatter than a water-rich, H_2 -dominated atmosphere with a solar abundance of water (oxygen) (Fig. 2). Flatness could indicate that the atmosphere has no scale height (see equation 1) (for example, due to a high mean molecular weight, μ), or herald the presence, yet again, of a thick haze layer obscuring the molecular features. Not surprisingly, a panchromatic obscuring haze layer is currently the front runner.

Lest one think that hazes completely mask the molecules of exoplanet atmospheres, Deming *et al.*⁴² have published transit spectra of HD 209458b (Fig. 3) and XO-1b that clearly show the water feature at around $1.4\ \mu\text{m}$. However, the expected accompanying water feature at about $1.15\ \mu\text{m}$ is absent. The best interpretation of this is that this feature is suppressed by the presence of a haze with a continuum, although wavelength-dependent, interaction cross-section that trails off at longer wavelengths. The weaker apparent degree of suppression in these exoplanet atmospheres might suggest that their hazes are thinner or deeper (at higher pressures) than in HD 189733b. Physical models explaining this behaviour are lacking.

So, the only atmospheric species that have clearly been identified in transit are water, sodium, potassium and a 'haze'. Molecular hydrogen is the only gas with a low enough μ to provide a scale height that is great enough to explain the detection in transit of any molecular features (see equation 1) in a hot, irradiated atmosphere, and I would include it as indirectly indicated. However, carbon monoxide, carbon dioxide, ammonia, nitrogen gas, acetylene, ethylene, phosphine, hydrogen sulphide, oxygen, ozone, nitrous oxide and hydrogen cyanide have all been proffered as exoplanet atmosphere gases. Clearly, the field is in its spectroscopic infancy. Facilities such as

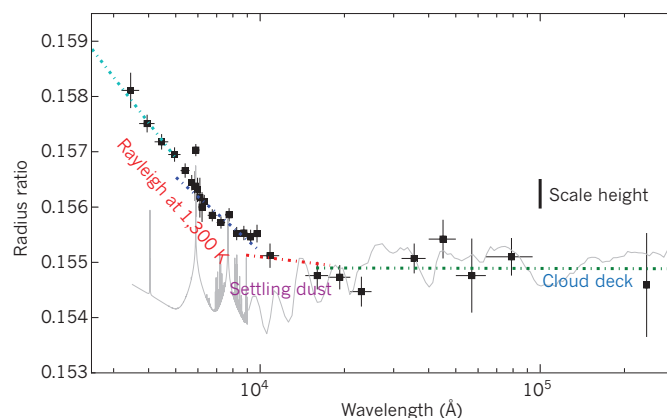


Figure 1 | Transit spectrum of giant exoplanet HD 189733b. The planet/star radius ratio against wavelength in ångströms. The black dots are the data points and the dotted lines are models. From left to right the dotted lines show the possible effect of Rayleigh scattering by mixed small grains at 2,000 K and at 1,300 K, by settling grains and by an opaque cloud deck. The grey line is an example spectrum without a haze. Reprinted with permission from ref. 36.

next-generation ground-based telescopes (extremely large telescopes, ELTs) and space-based telescopes such as the James Webb Space Telescope (JWST)²², or a dedicated exoplanet space-based spectrometer, will be essential if transit spectroscopy is to realize its true potential for exoplanet atmospheric characterization. The JWST in particular will have spectroscopic capability from ~ 0.6 to $\sim 28.3\ \mu\text{m}$ and will be sensitive to most of the useful atmospheric features expected in giant, Neptune-like and sub-Neptune exoplanets. It may also be able to detect and characterize a close-in Earth or super-Earth around a nearby small M star.

There are a number of theoretical challenges that must be met before transit data can be converted into reliable knowledge. Such spectra probe the terminator region of the planet that separates the day and night sides. They sample the transitional region between the hotter day and cooler night of the planet, at which the compositions may be changing and condensates may be forming. Hence, the compositions extracted may not be representative even of the bulk atmosphere. Ideally, one would want to construct dynamical three-dimensional (3D) atmospheric circulation models that couple non-equilibrium chemistry and detailed molecular opacity databases with multi-angle 3D radiation transfer. Given the emergence of hazes and clouds as potentially important features of exoplanet atmospheres, a meteorologically credible condensate model is also desired. We are far from the latter⁴³, and the former's capabilities are only now being constructed, with limited success⁴⁴. The dependence of transit spectra on species abundance is weak, making it now difficult to derive mixing ratios from transit spectra to better than a factor of 10 to 100. Although the magnitude of the variation of apparent radius with wavelength depends on atmospheric scale height, and hence temperature, the temperature–pressure profile and the variation of abundance with altitude are not easily constrained. To obtain even zeroth-order information, one frequently creates isothermal atmospheres with chemical equilibrium or uniform composition. Current haze models are ad hoc, and adjusted a posteriori to fit the all-too-sparse and at times ambiguous data. To justify the effort necessary to do better will require much improved and higher-resolution measured spectra⁵.

Data at secondary eclipse require a similar modelling effort, but probe the integrated flux of the entire dayside. Hence, a model that correctly incorporates the effects of stellar irradiation ('instellation') and limb effects is necessary. Moreover, the flux from the cooling planetary core, its longitudinal and latitudinal variation, and a circulation model that redistributes energy and composition are needed. Most models employed so far use a representative one-dimensional (planar) approximation, and radiative and chemical equilibrium for what is a

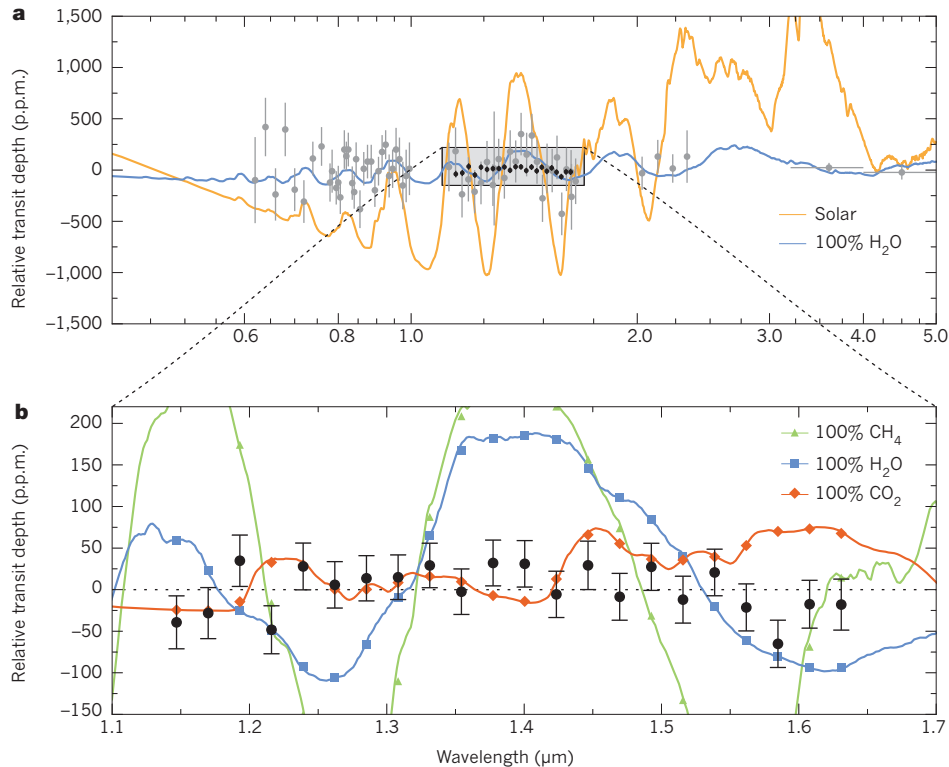


Figure 2 | The transmission spectrum of GJ 1214b. The relative depth of the transit of the sub-Neptune GJ 1214b against wavelength (1.1 μm to 1.7 μm). The coloured lines in both (a) and (b) are various transit spectral models without a haze (cloud-free solar composition, orange; 100% water, blue; methane, green; and carbon dioxide, red). The data (black and grey dots) are effectively flat, ruling out all models shown and suggesting a veiling haze.

hemispherical region that might be out of chemical equilibrium (and slightly out of radiative equilibrium). The emission spectra of the day-side depend more on the absorptive opacities, whereas transit spectra depend on both scattering and absorption opacities. Hence, if the haze inferred in some transit spectra is due predominantly to scattering, its effect on secondary eclipse spectra will be minimal, making it slightly more difficult to use insight gained from one to inform the modelling of the other.

Many giant exoplanets, and a few sub-Neptunes, have been observed at secondary eclipse, but the vast bulk of these data are comprised of a few photometric points per planet. The lion's share have been garnered using Spitzer, Hubble or large-aperture ground-based telescopes, and pioneering attempts to inaugurate this science were carried out by Deming *et al.*⁴⁵ and Charbonneau *et al.*⁴⁶. Photometry, particularly if derived using techniques that are subject to systematic errors, is ill-suited to delivering solid information on composition, thermal profiles or atmospheric dynamics. The most one can do with photometry at secondary eclipse is to determine rough average emission temperatures, and perhaps reflection albedos in the optical. Temperatures for close-in giant exoplanet atmospheres from around 1,000 to 3,000 K have, in this way, been determined. Of course, the mere detection of an exoplanet is a victory, and the efforts that have gone into winning these data should not be discounted. Nevertheless, with nearly 50 such campaigns and detections 'in the can', we have learned that it is only with next-generation spectra that use improved (perhaps dedicated) spectroscopic capabilities that the desired thermal and compositional information will be forthcoming.

One of the few reliable compositional determinations at secondary eclipse obtained so far is for the dayside atmosphere of HD 189733b using the now-defunct infrared spectrograph on-board Spitzer³⁹. This very-low-resolution spectrum nevertheless provided a 3σ detection of water at around 6.2 μm . Other papers have reported the detection of molecules at secondary eclipse, but many are less compelling, and earlier reports of water being detected using photometry alone

at secondary eclipse are very model-dependent⁴⁷. It is only with well-calibrated spectra that one can determine with confidence the presence in any exoplanet atmosphere of any molecule or atom.

Winds from planets

The existence of what are now somewhat contradictorily called hot Jupiters has, since the discovery of 51 Peg b in 1995, been somewhat of a puzzle. These planets probably cannot form as close as they are observed to their parent star and must migrate in, by some process, from beyond the so-called ice line. In such cold regions, ices can form and accumulate to nucleate gas-giant formation. Subsequent inward migration could be driven early in the planet's life by gravitational torquing by the protoplanetary disk or by planet–planet scattering, followed by tidal dissipation in the planet (which circularizes its orbit). However, once parked at between ~ 0.01 AU and 0.1 AU from the star, how does the gaseous planet, or a gaseous atmosphere of a smaller planet, survive evaporation by the star's intense irradiation during perhaps billions of years seemingly in extremis? The answer is that for sub-Neptunes and rocky planets their atmospheres or gaseous envelopes might not survive, but for more massive gas giants the gravitational well at their surfaces may be sufficiently deep. Nevertheless, since the first discoveries, evaporation has been of interest⁴⁸. The atmospheres of Earth and Jupiter are known to be evaporating, although at a very low rate. But what happens to a hot Jupiter that experiences 10^4 times the instellation that Jupiter does?

The answer came with the detection by Vidal-Madjar *et al.*⁴⁹ of a wind from HD 209458b. Using the transit method, but in the ultraviolet around the Lyman- α line of atomic hydrogen at around 0.12 μm , the authors measured a transit depth of about 15%. Such a large depth implies a planet radius greater than four R_p , which is not only much greater than what is inferred in the optical, but beyond the tidal Roche radius. Matter at such distances is not bound to the planet, and the only plausible explanation was that a wind was being blown off the planet. The absorption cross-sections in the ultraviolet are huge, so the matter densities that are necessary to generate a transverse chord optical depth

of one are very low — too low to affect the optical and infrared measurements. The upshot of this is the presence of a quasi-steady planetary wind with a mass-loss rate of 10^{10} – 10^{11} gm s⁻¹. At that rate, HD 209458b will lose no more than around 10% of its mass in Hubble time.

Since this initial discovery, winds from the hot Jupiters HD 189733b⁵⁰ and WASP-12b⁵¹, and from the hot Neptune GJ 436b⁵² have been discovered by the ultraviolet transit method and partially characterized. In all cases, the telltale indicator was in atomic hydrogen. Mass-loss rates have been estimated⁵³, and in the case of WASP-12b might be sufficient to completely evaporate the giant within as little as about 1 gigayear. The presence of atomic hydrogen implies the photolytic or thermal break-up of molecular hydrogen, so these data simultaneously suggest the presence of both H and H₂. Linsky *et al.*⁵⁴ detected ionized carbon and silicon in HD 209458b's wind, and Fossati *et al.*⁵¹ detected ionized magnesium in WASP-12b's wind, but the interpretation of the various ionized species detected in these transit-observation campaigns is ongoing.

The theoretical challenges posed by planetary winds revolve partly around the driver. Is the wind driven by the subset of the instellation represented by the ultraviolet and X-ray component of the total stellar flux? In addition, in the rotating system of the orbiting planet, what ingress or egress asymmetries in the morphology of the wind exist? There are indications that Coriolis forces on planet winds are indeed shifting the times of ingress and egress. What is the effect of planet–star wind interactions? There are suggestions of Doppler shifts in lines of the ultraviolet transit data that arise from planet-wind speeds, but how can we be sure? How is the material for the wind replenished from the planet atmosphere and interior? And finally, what is the correspondence between the ultraviolet photolytic chemistry in the upper reaches of the atmosphere that modifies its composition there and wind dynamics? This is a rich subject tied to many subfields of science, and is one of the important topics to emerge from transit spectroscopy.

Phase light curves and planet maps

As a planet traverses its orbit, its brightness, as measured at Earth at a given wavelength, varies with orbital phase. A phase light curve comprises both a reflected component that is a stiff function of the star–planet–Earth angle and is most prominent in the optical and ultraviolet; and a thermal component that more directly depends on the temperature and composition of the planet's atmosphere, and their longitudinal variation around the planet, and is most prominent in the near- and mid-infrared. Hence, a phase light curve is sensitive to the day–night contrast and is a useful probe of planetary atmospheres^{55–59}. It should be mentioned that the planet/star contrast ratio is largest for large exoplanets in the closest orbits, so hot Jupiters currently provide the best targets.

In the optical, there has been some work to derive the albedo^{55,56}, or reflectivity, of close-in exoplanets, which is largest when there are reflecting clouds and smallest when the atmosphere is absorbing. In the latter case, thermal emission at high atmospheric temperatures can be mistaken for reflection, so detailed modelling is required. In any case, Kepler, with its superb photometric sensitivity, has been used to determine optical phase curves⁶⁰ of a few exo-giants in the Kepler field, and the MOST (Microvariability and Oscillations of Stars) microsatellite has put a low upper limit on the optical albedo of HD 209458b^{61,62}, but much remains to be done to extract diagnostic optical phase curves and albedos for exoplanets.

Interesting progress has been made, however, in the thermal infrared. Using Spitzer at 8 μ m, Knutson *et al.*⁶³ not only derived a phase light curve for HD 189733b, but derived a crude thermal map of its surface. By assuming that the thermal emission pattern over the planet surface was fixed during the observations, they derived the day–night brightness contrast (translated into a brightness temperature at 8 μ m) and a longitudinal brightness temperature distribution. In particular, they measured the position of the 'hot spot'. If the planet is in synchronous rotation (spin period is the same as the orbital period), and there are no equatorial winds to advect heat around the planet, one would expect the hot spot to be at the substellar point. The light curve would phase

up with the orbit and the peak brightness would occur at the centre of secondary eclipse. However, what the authors observed was a shift downstream to the east by around $16^\circ \pm 6$. The most straightforward interpretation is that the stellar heat absorbed by the planet is advected downstream before being re-radiated by super-rotational flows such as those that are observed on Jupiter itself. Moreover, these data indicate that, because the measured day–night brightness temperature contrast was only about 240 K, the zonal wind flows driven by stellar irradiation carry heat to the night side, where it is radiated at a detectable level. Hence, these data point to the existence of atmospheric dynamics on HD 189733b, qualitatively (although not quantitatively) in line with theoretical expectations⁴⁴.

For HD 189733b, this work has been followed up using Spitzer at 3.6 μ m and 4.5 μ m⁶⁴ and, in a competing effort, a more refined map has been produced⁶⁵. Infrared phase curves for the giants HD 149026b⁶⁶, HAT-P-2b⁶⁷ and WASP-12b⁶⁸, among other exoplanets, have been obtained. However, one of the most intriguing phase curves was obtained by Crossfield *et al.*⁶⁹ using Spitzer at 24 μ m for the non-transiting planet ν Andromedae b (Fig. 4). The authors found a huge phase offset of around 80° , for which a cogent explanation is still lacking. The closeness of this planet to Earth could partly compensate for the fact that it is not transiting to allow sufficient photometric accuracy without eclipse calibration, yielding one of the few non-transiting light curves. All these efforts collectively demonstrate the multiple, at times unanticipated and creative, methods being employed by observers seeking to squeeze whatever information they can from exoplanets.

Theoretical models for light curves have been sophisticated, but theory and measurement have not yet meshed well. Both need to be improved. First, models need to be improved in terms of their treatment of hazes and clouds that could reside in exoplanet atmospheres and will boost reflection albedos significantly; second, they need to incorporate polarization to realize its diagnostic potential^{59,70}; third, they should constrain the possible range of phase functions to aid in retrievals; fourth, they need to embed the effects of variations in planet latitude and longitude in the analysis protocols; fifth, they should provide observational diagnostics with which to probe atmospheric pressure depths, particularly using multi-frequency data; sixth, they should be constructed as a function of orbital eccentricity, semi-major axis,

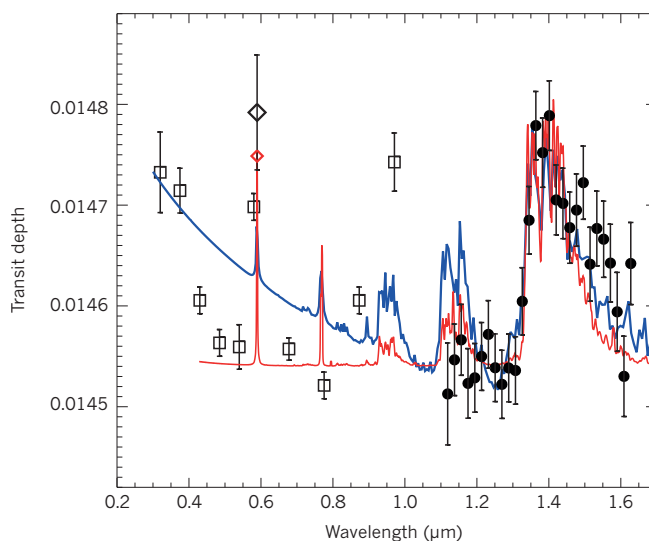


Figure 3 | Transit depth spectrum of the hot Jupiter HD 209458b. Data points are shown as black circles and open squares/diamonds. The presence of water is demonstrated by the occurrence of a feature at 1.4 μ m, but the corresponding ~ 1.15 - μ m feature is absent. The best explanation is that the latter is suppressed by haze scattering. Not obvious here is the fact that even the 1.4- μ m feature is muted with respect to non-haze models. The two coloured curves are representative model spectra with different levels of haze. Reprinted with permission from ref. 42.

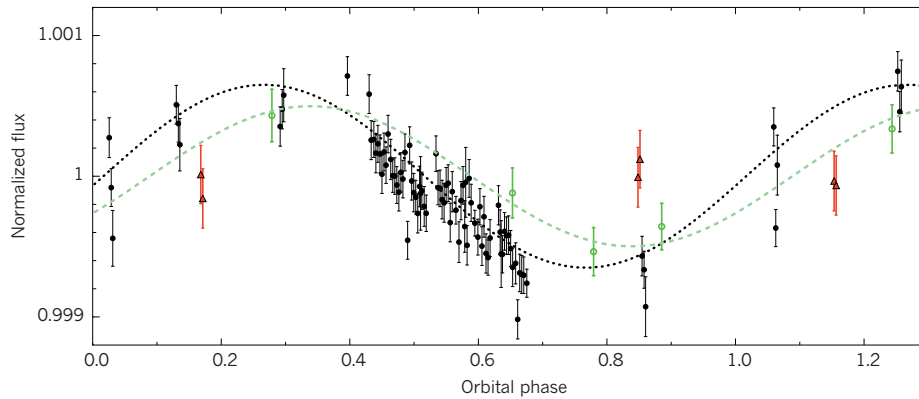


Figure 4 | The measured light curve of v Andromedae b. The thin black dotted curve is the authors' best fit to the data points (black dots with error bars at a wavelength of $24\ \mu\text{m}$), showing a phase offset of $\sim 80^\circ$ (22% of a circuit). Reprinted with permission from ref. 69.

and inclination; and finally they should span the wide range of masses and compositions that the heterogeneous class of exoplanets is likely to occupy. Accurate spectral data with good time coverage from the optical to the mid-infrared could be game-changing, but theory needs to be ready with useful physical diagnostics.

High spectral resolution techniques

The intrinsic dimness of planets under the glare of stars renders high-resolution, panchromatic spectral measurements difficult, if desirable. However, ultra-high spectral resolution measurements using large-aperture ground-based telescopes, but over a very narrow spectral range and targeting molecular band features in a planet's atmosphere that are otherwise jumbled together at lower resolutions, has recently been demonstrated. Snellen *et al.*⁷¹ have detected the Doppler variation owing to HD 209458b's orbital motion of carbon monoxide features near $\sim 2.3\ \mu\text{m}$. The required spectral resolution ($\lambda/\Delta\lambda$) was about 10^5 and the planet's projected radial velocity just before and just after primary transit changed from $+15\ \text{km s}^{-1}$ to $-15\ \text{km s}^{-1}$. This is consistent with the expected circular orbital speed of around $140\ \text{km s}^{-1}$ and provides

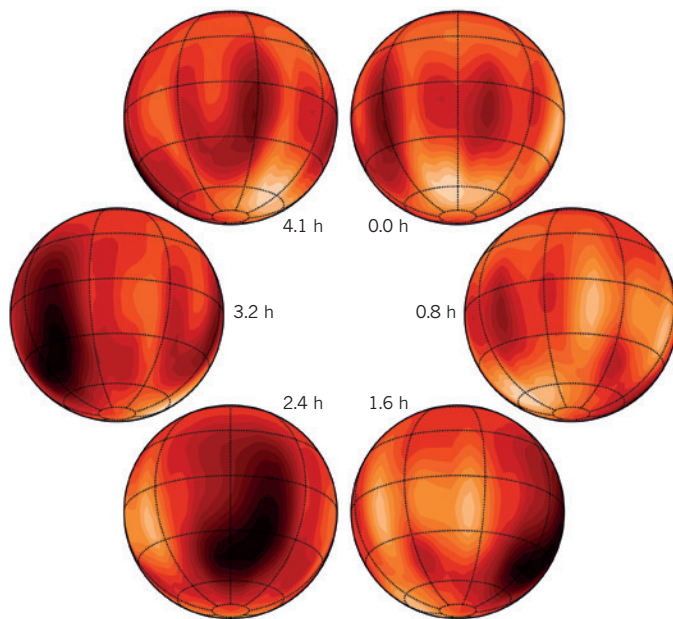


Figure 5 | Surface map of brown dwarf Luhman 16B. These maps are obtained by Doppler imaging and depict different epochs during the rotation of Luhman 16B. Large-scale cloud inhomogeneities are suggested by the dark patches at 2.4 hours and 3.2 hours. The rotation period of the brown dwarf is 4.9 hours. Reprinted with permission from ref. 76.

an unambiguous detection of carbon monoxide. Furthermore, this team attempted to measure the zonal wind speeds of air around the planet, estimated theoretically to be near $\sim 1\ \text{km s}^{-1}$, thereby demonstrating the potential of such a novel technique to extract weather features on giant exoplanets. The same basic method has been applied near primary transit to detect carbon monoxide⁷² and water⁷³ in HD 189733b. Carbon monoxide can be detected in Jupiter and was thermochemically predicted to exist in abundance in the atmospheres of hot Jupiters³¹, but its actual detection by this method is impressive.

In fact, the same technique has been successfully applied in the carbon monoxide band to the non-transiting planet τ Boötis b⁷⁴ and for the wide-separation giant planet (or brown dwarf) β Pictoris b⁷⁵, verifying the presence of carbon monoxide in both their atmospheres. Finally, using a related technique Crossfield *et al.*⁷⁶ have been able to conduct high-resolution 'Doppler imaging' of the closest known brown dwarf (Luhman 16B). By assuming that the brown dwarf's surface features are frozen during the observations and that it is in solid-body rotation, and by dividing the surface into a grid in latitude and longitude, they were able to determine (by model fitting) surface brightness variations from the variations of its flux and Doppler-shift time series. By this means, they mapped surface spotting that may reflect broken cloud structures (Fig. 5).

In support of such measurements, theory needs to refine its modelling of planet surfaces, zonal flows and weather features, 3D heat redistribution and velocity fields, and temporal variability. Currently, most 3D general circulation models do not properly treat high Mach number flows, but they predict zonal wind Mach numbers of order unity. There are suggestions that magnetic fields affect the wind dynamics and heating in the atmosphere, but self-consistent multi-dimensional radiation magnetohydrodynamic models have not yet been constructed.

This series of measurements of giant exoplanets and brown dwarfs using high-resolution spectroscopy focused on narrow molecular features emphasizes two important aspects of exoplanet research. The first is that observers can be clever and develop methods unanticipated in roadmap documents and decadal surveys. The second is that with the next-generation of ground-based ELTs equipped with impressive spectrometers, astronomers may be able to measure and map some exoplanets without using the high-contrast imaging techniques that are now emerging to compete.

High-contrast imaging

Before the successful emergence of radial-velocity and transit methods, astronomers expected that high-contrast direct imaging that separates out the light of the planet and of the star, and provides photometric and spectroscopic data for each, would be the leading means of exoplanet discovery and characterization. A few wide-separation brown dwarfs and/or super-Jupiter planets were detected by this means, but the yield was meagre. The fundamental problem is twofold: the planets

are intrinsically dim, and it is difficult to separate out the light of the planet from under the glare of the star for planet–star separations like those of the Solar System. Imaging systems need to suppress the stellar light scattered in the optics that would otherwise swamp the planet's signature. The planet/star contrast ratio for Jupiter is $\sim 10^{-9}$ in the optical and $\sim 10^{-7}$ in the mid-infrared. For Earth, the corresponding numbers are $\sim 10^{-10}$ and $\sim 10^{-9}$. These numbers are age, mass, orbital distance and star dependent, but demonstrate the challenge. Furthermore, contrast capabilities are functions of planet–star angular separation, restricting the orbital space that is accessible.

However, high-contrast imaging is finally emerging to complement other methods. It is most sensitive to wider-separation (~ 10 – 200 AU), younger giant exoplanets (and brown dwarfs), but technologies are coming online with which to detect older and less massive exoplanets down to around 1.0 AU separations for nearby stars (closer than ~ 10 parsecs)^{10–13,77}. Super-Neptunes around M dwarfs might soon be within reach. Using direct imaging, Marois *et al.*^{78,79} have detected four giant planets orbiting the A star HR 8799 (HR 8799b, HR 8799c, HR 8799d and HR 8799e) and Lagrange *et al.*⁸⁰ have detected a planet around the A star β Pictoris. The contrast ratios in the near infrared are about 10^{-4} , but capabilities near 10^{-5} have been achieved and performance near 10^{-7} is soon anticipated^{10,11}. One of the results to emerge from the measurements of both the HR 8799 and β Pictoris planets is that to fit their photometry in the near-infrared from ~ 1.0 to 3.0 μm , thick clouds, even thicker than those seen in L-dwarf brown dwarf atmospheres, are necessary⁸¹. This re-emphasizes the theme that the study of hazes and clouds (nephelometry) has emerged as a core topic in exoplanet studies.

One of the most exciting recent measurements through direct imaging was by Konopacky *et al.*⁸² of HR 8799c. Using the Ohio State Infrared Imager/Spectrometer (OSIRIS) on the 10-metre Keck II telescope, they obtained unambiguous detections between ~ 1.95 μm and 2.4 μm of both water and carbon monoxide in its $\sim 1,000$ K atmosphere. This $\lambda/\Delta\lambda = 4,000$ spectrum is one of the best obtained so far, but was enabled by the youth (around 30 million years), wide-angular separation and large mass (~ 5 – $10 M_J$) of the planet.

Improvements in theory that are needed to support direct imaging campaigns mirror those needed for light curves, but are augmented to include planet-evolution modelling to account for age, metallicity or composition and mass variations. Most high-contrast instruments are focused on the near-infrared, so cloud physics and near-infrared line lists for likely atmospheric constituents will require further work. The reader will note again that most observations and measurements of exoplanet atmospheres have been for giants. There are a few for sub-Neptunes and super-Earths, but high-contrast measurements of Earths around G stars like the Sun are not likely in the near future^{83,84}. The planet/star contrast ratios are just too low, although Earths around M stars might be within reach — if we get lucky. For now, giants and Neptunes are the focus, as astronomers hone their skills for an even more challenging future.

What we know about atmospheric compositions

The species we have, without ambiguity, discovered so far in exoplanet atmospheres are: water, carbon monoxide, sodium, potassium and hydrogen (H_2), with various ionized metals indicated in exoplanet winds. Expected, but as yet undetected, species include: ammonia, methane, nitrogen gas, carbon dioxide, hydrogen sulphide, phosphine, hydrogen cyanide, acetylene, ethylene, oxygen, ozone and nitrous oxide. The nature of the hazes and clouds inferred is as yet unknown. The atmospheres probed have temperatures from ~ 600 K to $\sim 3,000$ K. Good spectra are the essential requirements for unambiguous detection and identification of molecules in exoplanet atmospheres, and these have been rare. Determining abundances is also difficult, because to do so requires not only good spectra, but also reliable models. Errors in abundance retrievals of more than an order of magnitude are likely, and this fact has limited the discussion of abundances in this paper.

Nevertheless, with the construction of ground-based ELTs, the

various campaigns of direct imaging^{10–12}, the launch of the JWST, the possible launch of the 2.4 m Wide-Field Infrared Survey Telescope (WFIRST)-AFTA¹³, the various ongoing campaigns with Hubble and Spitzer, and with extant ground-based facilities, the near-term future of exoplanet atmospheric characterization promises to be even more exciting than its past. ■

Received 10 April; accepted 23 June 2014.

- Mayor, M. & Queloz, D. A Jupiter-mass companion to a solar-type star. *Nature* **378**, 355–359 (1995).
This discovery paper inaugurated the modern era of exoplanet research.
- Charbonneau, D., Brown, T., Latham, D. W. & Mayor, M. Detection of planetary transits across a Sun-like star. *Astrophys. J.* **529**, L45–L48 (2000).
- Borucki, W. J. *et al.* Kepler planet-detection mission: introduction and first results. *Science* **327**, 977–980 (2010).
- Moutou, C. *et al.* CoRoT: Harvest of the exoplanet program. *Icarus* **226**, 1625–1634 (2013).
- Burrows, A. S. Spectra as windows into exoplanet atmospheres. *Proc. Natl Acad. Sci. USA* <http://dx.doi.org/10.1073/pnas.1304208111> (2014)
This paper provides an unvarnished appraisal of current state-of-the-art exoplanet atmosphere characterization.
- Brown, T. Transmission spectra as diagnostics of extrasolar giant planet atmospheres. *Astrophys. J.* **553**, 1006–1026 (2001).
- Seager, S. & Sasselov, D. D. Theoretical transmission spectra during extrasolar giant planet transits. *Astrophys. J.* **537**, 916–921 (2000).
- Fortney, J. J. *et al.* On the indirect detection of sodium in the atmosphere of the transiting planet HD209458b. *Astrophys. J.* **589**, 615–622 (2003).
- Werner, M. W. *et al.* The Spitzer Space Telescope mission. *Astrophys. J.* **154** (Suppl.), 1–9 (2004).
- Macintosh, B. *et al.* The Gemini Planet Imager: from science to design to construction. *Proc. SPIE* **7015**, 701518 (2008).
- Beuzit, J.-L. *et al.* SPHERE: a planet finder instrument for the VLT. *Proc. SPIE* **7014**, 701418 (2008).
- Suzuki, R. *et al.* Performance characterization of the HiCIAO instrument for the Subaru Telescope. *Proc. SPIE* **7735**, 773530 (2010).
- Spergel, D. N. *et al.* Wide-field infrared survey telescope – astrophysics focused telescope assets WFIRST-AFTA final report. Preprint at <http://arxiv.org/abs/1305.5422> (2013).
- Madhusudhan, N., Knutson, H., Fortney, J. J. & Barman, T. Exoplanetary atmospheres. Preprint at <http://arxiv.org/abs/1402.1169> (2014).
- Burrows, A. & Orton, G. In *Exoplanets* (ed. Seager, S.) 419–440 (Univ. Arizona Press, 2010).
- Fletcher, L. N. *et al.* Exploring the diversity of Jupiter-class planets. *Phil. Trans. R. Soc. A* **372**, 20130064 (2014).
- Tinetti, G. Galactic planetary science. Preprint at <http://arxiv.org/abs/1402.1085> (2014).
- Tinetti, G. *et al.* in *Proc. Inter. Astronom. Union IAU Symposium 6* (S276) 359–370 (2011).
- Guillot, T. On the radiative equilibrium of irradiated planetary atmospheres. *Astron. Astrophys.* **520**, A27–A39 (2010).
- Burrows, A., Hubbard, W. B. & Lunine, J. I. The theory of brown dwarfs and extrasolar giant planets. *Rev. Mod. Phys.* **73**, 719–765 (2001).
- Burrows, A. *et al.* A nongray theory of extrasolar giant planets and brown dwarfs. *Astrophys. J.* **491**, 856–875 (1997).
- Deming, D. *et al.* Discovery and characterization of transiting super Earths using an all-sky transit survey and follow-up by the James Webb Space Telescope. *Publ. Astron. Soc. Pac.* **121**, 952–967 (2009).
- Rothman, L. S. *et al.* The HITRAN 2008 molecular spectroscopic database. *J. Quant. Spectrosc. Radiat. Transf.* **110**, 533–572 (2009).
- Tennyson, J. & Yurchenko, S. N. The status of spectroscopic data for the exoplanet characterisation missions. Preprint at <http://arxiv.org/abs/1401.4212> (2014).
- Hill, C., Yurchenko, S. N. & Tennyson, J. Temperature-dependent molecular absorption cross sections for exoplanets and other atmospheres. *Icarus* **226**, 1673–1677 (2013).
- Freedman, R. S., Marley, M. S. & Lodders, K. Line and mean opacities for ultracool dwarfs and extrasolar planets. *Astrophys. J.* **174** (Suppl.), 504–513 (2008).
- Sharp, C. M. & Burrows, A. Atomic and molecular opacities for brown dwarf and giant planet atmospheres. *Astrophys. J.* **168** (Suppl.), 140–166 (2007).
- Lodders, K. Solar System abundances and condensation temperatures of the elements. *Astrophys. J.* **591**, 1220–1247 (2003).
- Lodders, K. & Fegley, B. Atmospheric chemistry in giant planets, brown dwarfs, and low-mass dwarf stars. I. Carbon, nitrogen, and oxygen. *Icarus* **155**, 393–424 (2002).
- Lodders, K. & Fegley, B. *The Planetary Scientist's Companion* (Oxford Univ. Press, 1998).
- Burrows, A. & Sharp, C. Chemical equilibrium abundances in brown dwarf and extrasolar giant planet atmospheres. *Astrophys. J.* **512**, 843–863 (1999).
- Schaefer, L. & Fegley, B. Chemistry of silicate atmospheres of evaporating super-Earths. *Astrophys. J.* **703**, L113–L117 (2009).
- Lecavelier des Etangs, A., Pont, F., Vidal-Madjar, A. & Sing, D. Rayleigh scattering in the transit spectrum of HD 189733b. *Astron. Astrophys.* **481**, L83–L86 (2008).
- Charbonneau, D., Brown, T., Noyes, R. W. & Gilliland, R. L. Detection of an

- extrasolar planet atmosphere. *Astrophys. J.* **568**, 377–384 (2002).
This paper announced the first ever detection of a specific chemical species (sodium) in an exoplanet atmosphere.
35. Sing, D. K. *et al.* Gran Telescopio Canarias OSIRIS transiting exoplanet atmospheric survey: detection of potassium in XO-2b from narrowband spectrophotometry. *Astron. Astrophys.* **527**, 10 (2011).
36. Pont, F. *et al.* The prevalence of dust on the exoplanet HD 189733b from Hubble and Spitzer observations. *Mon. Not. R. Astron. Soc.* **432**, 2917–2944 (2013).
This paper is the most definitive study at primary transit pointing to the potential centrality of obscuring hazes in an exoplanet atmosphere.
37. Pont, F., Knutson, H. A., Gilliland, R. L. M. & Charbonneau D. Detection of atmospheric haze on an extrasolar planet: the 0.55–1.05 μ transmission spectrum of HD 189733b with the Hubble Space Telescope. *Mon. Not. R. Astron. Soc.* **385**, 109–118 (2008).
38. Burrows, A., Marley, M. M. & Sharp, C. M. The near-infrared and optical spectra of methane dwarfs and brown dwarfs. *Astrophys. J.* **531**, 438–446 (2000).
39. Grillmair, C. J. *et al.* Strong water absorption in the dayside emission spectrum of the planet HD 189733b. *Nature* **456**, 767–769 (2008).
40. Howe, A. & Burrows, A. Theoretical transit spectra for GJ 1214b and other ‘super-Earths’. *Astrophys. J.* **756**, 176–189 (2012).
41. Kreidberg, L. *et al.* Clouds in the atmosphere of the super-Earth exoplanet GJ1214b. *Nature* **505**, 69–72 (2014).
42. Deming, D. *et al.* Infrared transmission spectroscopy of the exoplanets HD 209458b and XO-1b using the Wide-Field Camera-3 on the Hubble Space Telescope. *Astrophys. J.* **774**, 95–112 (2013).
43. Marley, M. S., Ackerman, A. S., Cuzzi, J. N. & Kitzmann, D. In *Comparative Climatology of Terrestrial Planets* (eds Mackwell, S., Bullock, M. & Harder, J.) 367–391 (Univ. Arizona Press, 2013).
44. Showman, A. P. *et al.* Atmospheric circulation of hot Jupiters: coupled radiative-dynamical general circulation model simulations of HD 189733b and HD 209458b. *Astrophys. J.* **699**, 564–584 (2009).
45. Deming, D., Seager, S., Richardson, L. J. & Harrington, J. Infrared radiation from an extrasolar planet. *Nature* **434**, 740–743 (2005).
This paper was the first to demonstrate the potential of the Spitzer Space Telescope to measure the light of an exoplanet during secondary eclipse.
46. Charbonneau, D. *et al.* Detection of thermal emission from an extrasolar planet. *Astrophys. J.* **626**, 523–529 (2005).
47. Burrows, A., Hubeny, I. & Sudarsky, D. A theoretical interpretation of the measurements of the secondary eclipses of TrES-1 and HD 209458b. *Astrophys. J.* **625**, L135–L138 (2005).
48. Burrows, A. & Lunine, J. Astronomical questions of origins and survival. *Nature* **378**, 333 (1995).
49. Vidal-Madjar, A. *et al.* An extended upper atmosphere around the extrasolar planet HD209458b. *Nature* **422**, 143–146 (2003).
This paper was the first to discover signatures of winds emanating from exoplanets.
50. Lecavelier Des Etangs, A. *et al.* Evaporation of the planet HD 189733b observed in H I Lyman- α . *Astrophys. Astron.* **514**, 10 (2010)
51. Fossati, L. *et al.* Metals in the exosphere of the highly irradiated planet WASP-12b. *Astrophys. J.* **714**, L222–L227 (2010).
52. Kulow, J. R., France, K., Linsky, J. & Parke Loyd, R. O. Lyman- α transit spectroscopy and the neutral hydrogen tail of the hot Neptune GJ 436b. Preprint at <http://arXiv.org/abs/1403.6834> (2014).
53. Ehrenreich, D. & Désert, J.-M. Mass-loss rates for transiting exoplanets. *Astron. Astrophys.* **529**, A136 (2011).
54. Linsky, J. L. *et al.* Observations of mass loss from the transiting exoplanet HD 209458b. *Astrophys. J.* **717**, 1291–1299 (2010).
55. Marley, M. S., Gelino, C., Stephens, D., Lunine, J. I. & Freedman, R. Reflected spectra and albedos of extrasolar giant planets. I. Clear and cloudy atmospheres. *Astrophys. J.* **513**, 879–893 (1999).
56. Sudarsky, D., Burrows, A. & Pinto, P. Albedo and reflection spectra of extrasolar giant planets. *Astrophys. J.* **538**, 885–903 (2000).
This paper provides a comprehensive theory of the reflection and albedo spectra of giant exoplanets as a function of orbital distance and planet mass.
57. Burrows, A., Sudarsky, D. & Hubeny, I. Spectra and diagnostics for the direct detection of wide-separation extrasolar giant planets. *Astrophys. J.* **609**, 407–416 (2004).
58. Barman, T. S., Hauschildt, P. H. & Allard, F. Phase-dependent properties of extrasolar planet atmospheres. *Astrophys. J.* **632**, 1132–1139 (2005).
59. Madhusudhan, N. & Burrows, A. Analytic models for albedos, phase curves, and polarization of reflected light from exoplanets. *Astrophys. J.* **747**, 25–40 (2012).
60. Esteves, L. J., De Mooij, E. J. W. & Jayawardhana, R. Optical phase curves of Kepler exoplanets. *Astrophys. J.* **772**, 51–64 (2013).
61. Rowe, J. *et al.* The very low albedo of an extrasolar planet: MOST space-based photometry of HD 209458. *Astrophys. J.* **689**, 1345–1353 (2008).
62. Burrows, A., Ibgui, L. & Hubeny, I. Optical albedo theory of strongly-irradiated giant planets: the case of HD 209458b. *Astrophys. J.* **682**, 1277–1282 (2008).
63. Knutson, H. A. *et al.* A map of the day-night contrast of the extrasolar planet HD 189733b. *Nature* **447**, 183–186 (2007).
Using one of the first exoplanet light curves, this paper determined a crude surface temperature map of an exoplanet.
64. Knutson, H. A. *et al.* 3.6 and 4.6 μ phase curves and evidence for non-equilibrium chemistry in the atmosphere of extrasolar planet HD 189733b. *Astrophys. J.* **754**, 22–37 (2012).
65. Majeau, C., Agol, E. & Cowan, N. B. A. Two-dimensional map of the extrasolar planet HD 189733b. *Astrophys. J.* **747**, L20–L24 (2012).
66. Knutson, H. A. *et al.* The 8 μ phase variation of the hot Saturn HD 149026b. *Astrophys. J.* **703**, 769–784 (2009).
67. Lewis, N. K. *et al.* Orbital phase variations of the eccentric giant planet HAT-P-2b. *Astrophys. J.* **766**, 95–117 (2013).
68. Cowan, N. B. *et al.* Thermal phase variations of WASP-12b: defying predictions. *Astrophys. J.* **747**, 82–98 (2012).
69. Crossfield, I. J. M. *et al.* A new 24 μ phase curve for u Andromedae b. *Astrophys. J.* **723**, 1436–1446 (2010).
70. Seager, S., Whitney, B. A. & Sasselov, D. D. Photometric light curves and polarization of close-in extrasolar giant planets. *Astrophys. J.* **540**, 504–520 (2000).
71. Snellen, I. A. G., de Kok, R. J., de Mooij, E. J. W. & Albrecht, S. The orbital motion, absolute mass and high-altitude winds of exoplanet HD 209458b. *Nature* **465**, 1049–1051 (2010).
72. de Kok, R., *et al.* Detection of carbon monoxide in the high-resolution day-side spectrum of the exoplanet HD 189733b. *Astron. Astrophys.* **554**, A82 (2013).
73. Birkby, J. *et al.* Detection of water absorption in the day side atmosphere of HD 189733b using ground-based high-resolution spectroscopy at 3.2 μ . *Mon. Not. R. Astron. Soc.* **436**, L35–L39 (2013).
74. Brogi, M. *et al.* The signature of orbital motion from the dayside of the planet τ Boötis b. *Nature* **486**, 502–504 (2012).
75. Snellen, I. A. G. *et al.* The fast spin-rotation of the young extra-solar planet β Pictoris b. *Nature* **509**, 63–65 (2014).
76. Crossfield, I. J. M. *et al.* A global cloud map of the nearest known brown dwarf. *Nature* **505**, 654–656 (2014).
77. Burrows, A. A theoretical look at the direct detection of giant planets outside the Solar System. *Nature* **433**, 261–268 (2005).
78. Marois, C. *et al.* Direct imaging of multiple planets orbiting the star HR 8799. *Science* **322**, 1348–1352 (2008).
This paper represents the coming of age of the direct, high-contrast imaging technique of exoplanet discovery and characterization.
79. Marois, C., Zuckerman, B., Konopacky, Q. M., Macintosh, B. & Barman, T. Images of a fourth planet orbiting HR 8799. *Nature* **468**, 1080–1083 (2010).
80. Lagrange, A. M. *et al.* A probable giant planet imaged in the β Pictoris disk. VLT/NaCo deep L'-band imaging. *Astron. Astrophys.* **493**, L21–L25 (2009).
81. Madhusudhan, N., Burrows, A. & Currie, T. Model atmospheres for massive gas giants with thick clouds: application to the HR 8799 planets. *Astrophys. J.* **737**, 34–48 (2011).
82. Konopacky, Q. M., Barman, T. S., Macintosh, B. A. & Marois, C. Detection of carbon monoxide and water absorption lines in an exoplanet atmosphere. *Science* **339**, 1398–1401 (2013).
83. Kaltenegger, L., Traub, W. A. & Jucks, K. W. Spectral evolution of an Earth-like planet. *Astrophys. J.* **658**, 598–616 (2007).
84. Ehrenreich, D., Tinetti, G., Lecavelier Des Etangs, A., Vidal-Madjar, A. & Selsis, F. The transmission spectrum of Earth-size transiting planets. *Astron. Astrophys.* **448**, 379–393 (2006).

Acknowledgements The author acknowledges support in part under Hubble Space Telescope grants HST-GO-12181.04-A, HST-GO-12314.03-A, HST-GO-12473.06-A, and HST-GO-12550.02 and Jet Propulsion Laboratory/Spitzer Agreements 1417122, 1348668, 1371432, 1377197 and 1439064.

Author Information Reprints and permissions information is available at www.nature.com/reprints. The author declares no competing financial interests. Readers are welcome to comment on the online version of this paper at go.nature.com/2e7lmg. Correspondence should be addressed to A.S.B. (burrows@astro.princeton.edu).